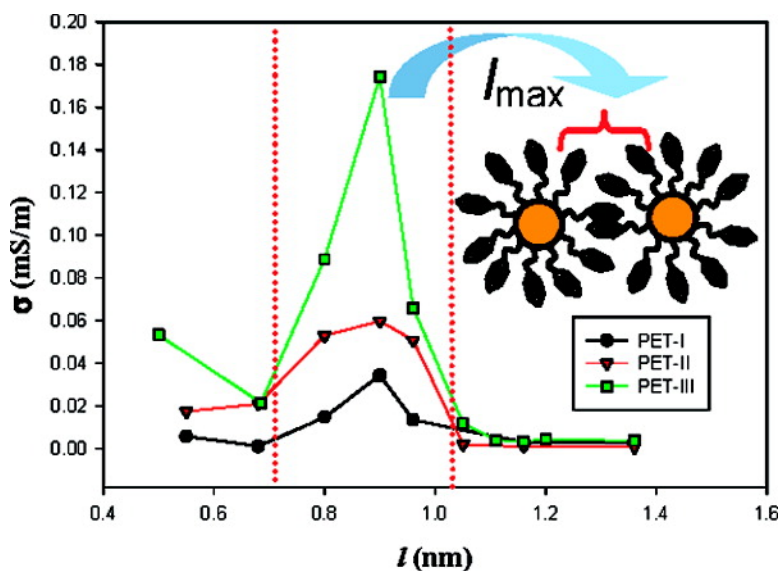


Interparticle Charge Transfer Mediated by π - π Stacking of Aromatic Moieties

Sulolit Pradhan, Debraj Ghosh, Li-Ping Xu, and Shaowei Chen

J. Am. Chem. Soc., **2007**, 129 (35), 10622-10623 • DOI: 10.1021/ja072597p • Publication Date (Web): 16 August 2007

Downloaded from <http://pubs.acs.org> on February 15, 2009



More About This Article

Additional resources and features associated with this article are available within the HTML version:

- Supporting Information
- Links to the 4 articles that cite this article, as of the time of this article download
- Access to high resolution figures
- Links to articles and content related to this article
- Copyright permission to reproduce figures and/or text from this article

[View the Full Text HTML](#)

Interparticle Charge Transfer Mediated by π - π Stacking of Aromatic Moieties

Sulolit Pradhan, Debraj Ghosh, Li-Ping Xu, and Shaowei Chen*

Department of Chemistry and Biochemistry, University of California, Santa Cruz, California 95064

Received April 13, 2007; E-mail: schen@chemistry.ucsc.edu

Lately intense research interests have been focused on the electronic conductivity properties of transition-metal nanoparticles (e.g., Au, Pd, and Ag) that are passivated by an organic monolayer (i.e., the so-called monolayer-protected nanoparticles).¹ With such a core-shell composite nanostructure, the resulting conductivity can be tailored by the combined effects of the conductive inorganic cores and the insulating organic shells, where the cores dictate the Coulomb blockade characteristics while the organic shells serve as the insulating barrier of interparticle charge transfer.² In addition, the collective conductivity properties of their organized assemblies are found to be determined not only by the particle chemical structure (core size, shape, and surface ligands) but also by the specific chemical environments and interparticle interactions as well.²

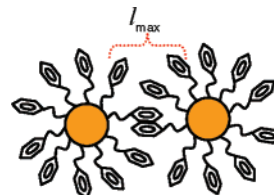
Toward this end, electrochemistry has been a powerful tool in the evaluation of the electronic conductivity of nanoparticle solids. In particular, in conjunction with the Langmuir and Langmuir-Blodgett (LB) techniques, one can readily manipulate the interparticle separation and concurrently examine the particle ensemble conductance, leading to the establishment of an unambiguous correlation between the particle ensemble structure and conductivity properties, in contrast to dropcast thick films.³⁻⁵

For instance, Heath and co-workers⁶ studied the electrical characteristics of a Langmuir monolayer of alkanethiolate-protected silver (AgSR) nanoparticles at the air-water interface by examining the corresponding linear and nonlinear ($\chi^{(2)}$) optical responses and observed a transition from insulator to metal when the interparticle spacing was sufficiently small. Such a transition was also manifested in electrochemical impedance measurements.⁶ Using scanning electrochemical microscopy (SECM), Bard et al.⁷ also observed a similar metal-insulator transition of AgSR nanoparticle monolayers at the air-water interface by monitoring the feedback currents at varied surface pressures (and interparticle separations). More recently, we observed that by deliberate control of the nanoparticle structures and interparticle interactions, single electron-transfer could also be achieved in LB thin films of monodisperse gold nanoparticles.⁸

Yet, these earlier studies are mostly focused on nanoparticles passivated by an alkanethiolate monolayer; and effects of aromatic functional groups on the interparticle charge transfer have remained largely unexplored. Murray and co-workers³ examined the conductivity properties of dropcast thick films of a series of gold nanoparticles with varied arene-thiolate protecting shells and observed that the tunneling barriers of interparticle charge-transfer predominantly arose from the saturated segment of the organic capping ligands.

In this report, we investigated the electronic conductivity of LB monolayers of phenylethylthiolate-passivated gold (PET-Au) nanoparticles that were prepared at varied surface pressures (interparticle separations) and observed that the π - π stacking of the phenyl moieties from neighboring particles, which was manipulated by the Langmuir technique, played a critical role in the regulation of interparticle charge transfer. At interparticle separation

Scheme 1



where the phenyl moieties from adjacent particles were fully stacked, the interparticle conductance reached the maximum (Scheme 1). This may be exploited as a sensitive mechanism to mediate interparticle charge transfer.

The PET-Au particles were synthesized by adopting a literature synthetic protocol,⁹ with core diameters varied at 1.39 ± 0.73 nm (PET-I), 1.64 ± 0.79 nm (PET-II), and 2.97 ± 0.62 nm (PET-III), as determined by transmission electron microscopic measurements (Figure S1, Supporting Information). The monolayer films of these nanoparticles were first prepared by spreading a calculated amount of the particle solutions in toluene onto the water surface of an LB trough (NIMA 611D, a representative Langmuir isotherm was included as Figure S3) and then deposited onto an interdigitated arrays electrode (IDA, consisting of 25 pairs of gold fingers, $5 \mu\text{m} \times 5 \mu\text{m} \times 3$ mm, from ABTECH) by the LB method at varied interparticle separations. Structural integrity of the nanoparticle monolayers was examined by TEM and STM measurements where the interparticle separations were found to be in good agreement with the estimations based on the Langmuir isotherm (Tables S1 and S2). Electrochemical measurements were then carried out with an EG&G PARC 283 potentiostat/galvanostat in vacuo with a cryostat from Janis Research and at different temperatures (Lake-shore 331 temperature controller).

Insets of Figure 1 show some representative current-potential (I - V) profiles of the LB monolayers of the three nanoparticles synthesized above within the temperature range of 100 to 320 K. It can be seen that the I - V responses all exhibit linear (ohmic) behaviors, indicative of relatively strong interparticle electronic coupling, most probably as a result of the short ligand chains and aromatic moieties that facilitate interparticle charge transfer.³ In addition, the ensemble conductivity, as evaluated from the slope of the I - V profiles, increases with increasing particle core size, which can be accounted for by the enhanced interparticle dipolar interactions.^{10,11} The conductivity is also found to increase with increasing temperature, consistent with the semiconductor characteristics of the nanoparticles which are essentially nanoscale organic-inorganic composite materials. Also the temperature dependence of the ensemble conductivity exhibits a clear Arrhenius behavior at temperatures greater than or equal to 280 K (Figure S6), suggestive of a thermal activation mechanism for the interparticle charge-transfer driven by electron hopping.³

More interestingly, the ensemble conductivity (Figure 1) exhibits a volcano-shaped dependence on the interparticle separation for all three particles within the entire temperature range. This deviates drastically from our previous study¹² of Langmuir monolayers of

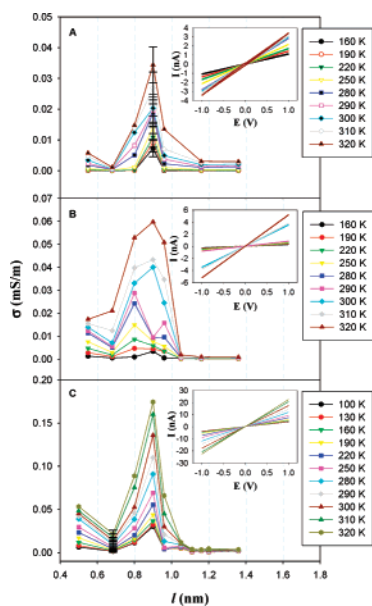


Figure 1. Variation of nanoparticle monolayer conductivity (σ) with interparticle edge-to-edge separation (l) at different temperatures for three PET–Au particles: (A) PET-I, (B) PET-II, and (C) PET-III. Error bars reflect statistical average of at least three measurements. Insets show the representative I – V profiles of the corresponding nanoparticles at $l = 0.90$ nm. Potential scan rate, 20 mV/s.

gold nanoparticle passivated by saturated alkanethiolates where the particle conductivity was found to exhibit an exponential decay with increasing interparticle separation. From Figure 1, one can see that the maximum conductivity corresponds to a narrow range of interparticle edge-to-edge distances (l) of ca. 0.8–1.0 nm. Note that in nanoparticle solids, ligand intercalation and hence the van der Waals (vdW) interactions between the ligands of adjacent particles play an important role in the determination of the energetic barrier for interparticle electron hopping. That is, the interparticle charge-transfer most probably consists of both through-bond and through-space (by way of the vdW contacts between interdigitated ligands) contributions. Thus, it can be envisioned that in the present study, the ligand vdW interactions will be enhanced by the π – π stacking of the phenyl moieties from adjacent particles. In fact, on the basis of Hyperchem calculations of the fully extended ligand chains, the interparticle edge-to-edge separation is anticipated to be ca. 1.11 nm when the phenyl rings are fully overlapped (Scheme 1; note that the phenyl ring is 0.28 nm in diameter and the optimal range of l is 0.8–1.0 nm, Figure 1). This is somewhat longer than the interparticle separation observed in Figure 1 for maximum ensemble conductance ($l_{\max} = 0.9$ nm for all three PET–Au particles within the entire temperature range under study). This may be, at least in part, ascribed to the tilting conformation of the ligands adsorbed onto the gold core surface. Furthermore, in reality the stacking of the phenyl moieties from neighboring particles may deviate somewhat from the ideal parallel configuration.

The mediation of interparticle charge transfer by π – π stacking of the aromatic moieties may also account for the substantially larger conductivity observed at l_{\max} with the nanoparticle monolayers than with their respective dropcast thick films (Figures S8), although the overall I – V responses are very similar (Figure S7). In dropcast films of alkanethiolate-protected nanoparticles, it is generally believed that the capping ligands between neighboring particles are fully intercalated.^{4,5} Yet, for arenethiolate-protected gold nanoparticles, Murray et al.³ proposed a model based on ligand head-to-head contacts to account for the solid-state electronic conductivity. For the PET–Au particles, this corresponds to $l = 1.36$ nm. From

Figure 1, it can be seen that this interparticle distance lies beyond the optimal range for maximum ensemble conductivity.

When compared to the monolayer conductivity at similar interparticle separation ($l = 1.36$ nm), the dropcast films (Figure S8) exhibit interesting variation of the conductivity with particle core size. For the smallest PET-I particles, the dropcast films exhibit a conductivity about 2 orders of magnitude smaller than the LB monolayers; for the larger PET-II particles, the monolayer conductivity becomes only several folds larger than that of the dropcast films; whereas for the largest PET-III particles, it is the opposite, the dropcast films now show a conductivity a few times that of the LB monolayers. This suggests that for smaller particles, the particle arrangements within the multilayer ensembles play a predominant role in the determination of the overall conductivity, whereas for larger particles, the enhanced contributions from interparticle dipolar (electronic) interactions become increasingly appreciable.^{10,11}

Furthermore, from the temperature dependence of the ensemble conductivity (Figure S8), one can see that the smaller the particle core size is, the steeper is the change of the conductivity with increasing temperature. Recently Murray et al.¹³ showed that thermally induced core motion led to drastic enhancement of the electronic conductivity of nanoparticle solids. It is anticipated that the core thermal motion will be stronger for smaller particles, consistent with the above experimental observations (Figure S8).

It has been recognized that the particle ensemble conductivity is the combined consequence of the interplay of at least three effects:² (i) the disorder due to the dispersity of particle core size, shape and chemical environments, (ii) the dipole coupling between adjacent particles, and (iii) the Coulomb repulsion of electrons (of opposite spins) on a given particle. The present study strongly suggests that the interparticle charge transfer can also be sensitively mediated by the vdW interactions between the functional moieties of the organic capping ligands from adjacent particles. Note that electron transport along a carbon nanotube telescope has also been found to exhibit an oscillation with the displacement of the outer tube relative to the inner tube, which is attributable to the periodic interwall π – π coupling.¹⁴ Such a controlling mechanism may be exploited for nanoscale sensing and switching applications.

Acknowledgment. This work was supported in part by the NSF (Grants CHE-0456130 and 0718170), and ACS–PRF (Grant 39729-AC5M).

Supporting Information Available: Additional experimental details and data analyses (Figures S1 to S8). This material is available free of charge via the Internet at <http://pubs.acs.org>.

References

- (1) Brust, M.; Walker, M.; Bethell, D.; Schiffrin, D. J.; Whyman, R. *J. Chem. Soc., Chem. Commun.* **1994**, 801.
- (2) Remacle, F.; Levine, R. D. *Chemphyschem* **2001**, *2*, 20.
- (3) Wuelfing, W. P.; Murray, R. W. *J. Phys. Chem. B* **2002**, *106*, 3139.
- (4) Wang, L. Y.; Shi, X. J.; Kariuki, N. N.; Schadt, M.; Wang, G. R.; Rendeng, Q.; Choi, J.; Luo, J.; Lu, S.; Zhong, C. J. *J. Am. Chem. Soc.* **2007**, *129*, 2161.
- (5) Ibanez, F. J.; Gowrishetty, U.; Crain, M. M.; Walsh, K. M.; Zamborini, F. P. *Anal. Chem.* **2006**, *78*, 753.
- (6) Collier, C. P.; Vossmeier, T.; Heath, J. R. *Annu. Rev. Phys. Chem.* **1998**, *49*, 371.
- (7) Quinn, B. M.; Prieto, I.; Haram, S. K.; Bard, A. J. *J. Phys. Chem. B* **2001**, *105*, 7474.
- (8) Pradhan, S.; Sun, J.; Deng, F.; Chen, S. W. *Adv. Mater.* **2006**, *18*, 3279.
- (9) Donkers, R. L.; Lee, D.; Murray, R. W. *Langmuir* **2004**, *20*, 1945.
- (10) Remacle, F.; Levine, R. D. *Isr. J. Chem.* **2002**, *42*, 269.
- (11) Snow, A. W.; Wohltjen, H. *Chem. Mater.* **1998**, *10*, 947.
- (12) Chen, S. W. *Anal. Chim. Acta* **2003**, *496*, 29.
- (13) Choi, J. P.; Coble, M. M.; Branham, M. R.; DeSimone, J. M.; Murray, R. W. *J. Phys. Chem. C* **2007**, *111*, 3778.
- (14) Grace, I. M.; Bailey, S. W.; Lambert, C. J. *Phys. Rev. B* **2004**, *70*, 153405.

JA072597P